Mechanisms of dopant impurity diffusion in silicon

C. S. Nichols, C. G. Van de Walle,* and S. T. Pantelides
IBM Research Division, Thomas J. Watson Research Center, P.O. Box 218, Yorktown Heights, New York 10598
(Received 20 April 1989)

We present a comprehensive investigation of dopant diffusion in silicon under equilibrium and nonequilibrium concentrations of intrinsic point defects. Using first-principles total-energy calculations combined with available experimental data, we seek to resolve a series of outstanding controversies regarding the diffusion mechanisms of B, P, As, and Sb in silicon. We find that, under equilibrium conditions, vacancies and interstitials mediate the diffusion of all dopants with comparable activation energies, except Sb, for which the interstitial component has a high activation energy. Under nonequilibrium conditions, e.g., under injection of excess point defects, we derive the relevant expressions for the activation energy for a variety of possible diffusion mechanisms and injection conditions. Under oxidation, the calculated values are in excellent agreement with the available experimental data. In addition, theory and experiment suggest that the concerted exchange mechanism, involving no point defects, plays only a minor role in dopant diffusion.

I. INTRODUCTION

Diffusion of impurity or host atoms through crystalline solids has been studied extensively for many years.[1,2] There are two basic types of mechanisms by which substitutional dopant impurities can diffuse. Diffusion can be mediated either by native point defects, such as vacancies and self-interstitials, or by an intrinsic mechanism that occurs spontaneously (i.e., in the absence of defects) in the bulk. In addition, there have been some suggestions that "extended defects" may play a role in high-temperature diffusion processes.[3] While experimental and theoretical approaches have considered these atomistic mechanisms of diffusion, most evidence for or against a particular mechanism has been indirect; for example, the comparison between an impurity profile measured experimentally and one derived analytically or numerically. In recent years, however, both experimental and theoretical tools have been developed with which diffusion can be studied from a microscopic, atomistic viewpoint directly. Despite these advances, there is no general consensus regarding the relative contributions of the various mechanisms to impurity diffusion.

It has been observed that a number of surface processing conditions[4] alter the bulk point-defect concentration in Si. Oxidation, for example, has been shown to inject excess self-interstitials, while nitridation of the surface injects excess vacancies.[5] Although the details of such processes are not completely understood, measurement of dopant diffusion coefficients under equilibrium concentrations of point defects and under oxidation or nitridation conditions affords the possibility of discriminating between the mechanisms responsible for dopant diffusion. However, the theories underlying the interpretation of such experiments are incomplete, relying for the most part on assumptions whose validity is uncertain.[6] For example, in oxidation experiments, Antoniadis and Moskowitz[7] observed that the P diffusion coefficient is enhanced with respect to its equilibrium value. They concluded that P diffuses via a *dual vacancy-interstitial mechanism,* although the microscopics of the interstitial mechanism were not specified. Also under interstitial injection, Fahey *et al.*[8] found an identical P diffusion enhancement. However, under injection of excess vacancies they observed a retardation of the P diffusion coefficient with respect to its equilibrium value. From these two experiments, they concluded that P diffusion is almost *exclusively mediated by self-interstitials.* No attempt has been made to assess the contribution of any intrinsic mechanism in these experiments.

Numerical solution of the coupled system of equations governing diffusion in Si offers relatively inexpensive and quick insight into possible mechanisms. However, the complexity of the relevant equations has made solution of the full problem unfeasible, and the consequent simplifying assumptions made are often unrealistic.[9,10] In one such simulation, the authors concluded that P diffuses exclusively by a *vacancy* mechanism,[11] in conflict with the nonequilibrium experimental conclusions above.

First-principles calculations have also recently addressed the problem of impurity diffusion pathways and mechanisms.[12,13] The work of Ref. 12 considered only the migration of aluminum as an interstitial and did not address the issue of a vacancy mechanism. The work of Ref. 13 focused on equilibrium conditions and considered defect-mediated mechanisms. This work established that native *point* defects mediate impurity diffusion with activation energies comparable to experimental values, obviating the need for "extended defects." No definitive conclusion was reached in this work regarding the dominance of one point-defect species over the other, however. Finally, although thorough first-principles calculations have demonstrated that a concerted exchange (CE) mechanism is energetically comparable to defect mechanisms for self-diffusion,[14] no quantitative support that this mechanism is relevant for dopant impurity diffusion has been offered. An excellent overview of the various experiments, simulations, and theoretical calculations probing

dopant diffusion is given in the review by Fahey *et al.*[15]

We recently published a brief account of an extensive theoretical study of dopant diffusion mechanisms in Si.[16] In this paper, we give a more extensive and detailed exposition of that work. In particular, we use first-principles state-of-the-art calculations to investigate vacancy-, interstitial-, and CE-mediated diffusion pathways of substitutional B, P, As, and Sb in Si. Activation energies for equilibrium conditions are calculated and compared to available experimental work. In addition, we discuss a systematic framework for impurity diffusion under nonequilibrium concentrations of point defects. Expressions for the activation energies of diffusion in terms of theoretically and experimentally available numbers are found and predictions for the expected form of the diffusion coefficient are given. Using these results, in conjunction with available experimental data, we can discriminate between the different mechanisms. We find that P, As, and B diffusion have substantial interstitial components, while Sb diffusion is vacancy dominated. Theoretical results and experimental data suggest that the CE mechanism has a limited role in dopant diffusion. In large part, we confirm the picture advocated by Fahey and co-workers[8] with regard to the point-defect mechanisms.

II. METHODOLOGY

Our calculations are based on Hohenberg-Kohn density-functional theory, the Kohn-Sham local-density approximation (LDA) for exchange and correlation,[17] and norm-conserving pseudopotentials[18] for the electron-ion interaction. The relevant Schrödinger equation is solved to obtain the total energy by a momentum-space formalism[19] in a supercell geometry.[20] We describe the essential aspects of this methodology below. A useful and more comprehensive discussion can also be found in a recent review by Pickett.[21]

For the electron-electron interactions, density-functional theory, within the LDA, is utilized. The LDA consists of the assumption that the exchange and correlation energy at a point **r** is a function of the electron density only at **r**. The approximation is considered valid for systems with slowly varying electron densities. In practice, in semiconductors the LDA has proven remarkably successful. But it is by now well known that the LDA predicts conduction-band states and levels derived mostly from conduction-band states to be too low in energy. This is the major source of error in the methodology.

The pseudopotentials used in our calculations are generated according to the Hamann-Schlüter-Chiang scheme.[18] More details concerning the specifics of the Si potential and results of test calculations carried out for this potential are given in Ref. 22. For B impurities, we use a pseudopotential first discussed by Denteneer *et al.*[23] The cutoff radii of the B pseudopotential were adjusted so as to minimize the basis-set size, but still faithfully describe the properties of B impurities in Si. The convergence properties of this pseudopotential are fully discussed in Ref. 23. For the donor impurities treated here, P, As, and Sb, we used the pseudopotentials as tabulated by Bachelet, Hamann, and Schlüter.[24]

The solution of the relevant Schrödinger equation in a supercell geometry has been extensively exploited in many calculations, including superlattice geometries, defects, and amorphous semiconductors. In the present work, we follow the methodology of Bar-Yam and Joannopoulos[20] for combining density-functional theory and the pseudopotential approximation in a supercell framework. The supercell approach artificially introduces periodicity by translating a unit cell, which contains the defect or impurity, along its three direct-lattice vectors until all of space is filled. Convergence of the unit-cell size is achieved when the defects in neighboring cells interact by less than some desired tolerance (as manifested by the dispersion of the defect levels). Furthermore, enough neighbors of the impurity are required so as to obtain accurate relaxations. For example, an impurity atom at the bond-center (BC) position causes a large disruption of the crystalline network such that relaxation of at least two shells of neighbors are important.

The wave functions and potentials are expanded in a plane-wave basis. Convergence of the basis-set size was extensively and thoroughly tested. Plots of the total-energy difference between As impurities in two different sites in the crystal are shown in Fig. 1. Figure 1(a) shows

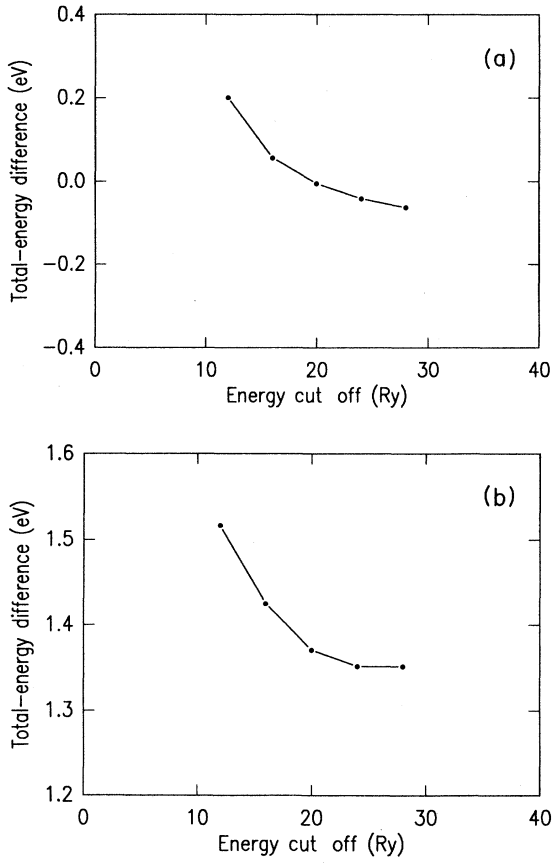

FIG. 1. Convergence of the total-energy differences in an 8-atom supercell as a function of the basis-set cutoff energy. (a) Total-energy difference between As at the T and H sites. (b) Total-energy difference between As at the BC and T sites.

the total-energy difference between a neutral As atom at the high-symmetry tetrahedral (T) and hexagonal (H) sites as a function of the energy cutoff. The calculations were performed in an 8-atom supercell, which is sufficient for basis-set–convergence studies. The abscissa is the kinetic energy E of the plane waves used in diagonalizing the Hamiltonian. The points plotted are for the highest-energy plane waves included in any basis set; plane waves from 0 to $E/2$ are utilized in the exact diagonalization process, while those between $E/2$ and E are treated in second-order Löwdin perturbation theory.[25] We introduce the notation $(E_1;E_2)$ to indicate the two energy cutoffs. From Fig. 1(a) we conclude that the total-energy difference has achieved convergence at a cutoff of (10;20) Ry to within 0.05 eV of its final value. We have also tested the Löwdin perturbation theory for this particular total-energy difference by computing the total energy at the cutoff (20;20) Ry. Results of these calculations show that at (10;20) Ry, the additional plane waves cause deviations only on the order of 0.03 eV.

Figure 1(b) depicts a somewhat different test case. The total-energy difference between neutral As at the T and (BC) sites is shown. At a cutoff of (10;20) Ry, the total-energy difference is within 0.02 eV of its fully converged value. Test calculations have also been performed in 16- and 32-atom cells [up to (12;24) Ry] and show that the cutoff (10;20) Ry is sufficient for reliable conclusions. We have also performed similar tests for P and Sb and observe that these impurities have convergence properties analogous to As.

We have performed supercell-size convergence tests for all impurities in 8-, 16-, and 32-atom cells. The maximum error in total-energy differences encountered in scaling from 16- to 32-atom cells is found to be 0.3 eV for P, As, and Sb impurities in Si. For B impurities, the maximum change in total-energy differences between any two atomic configurations is much smaller, only 0.1 eV. We therefore use 32-atom cells throughout these calculations, such that the distance between defects in neighboring cells is 9.4 Å.

Integrations over the Brillouin zone to obtain the charge density are performed using a special-points scheme. The special points are generated according to the algorithm of Monkhorst and Pack.[26] In 32-atom cells, a sampling of two special points has proven adequate for high-symmetry configurations. Lower-symmetry configurations require a larger, but equivalent, set.

Unless otherwise explicitly stated, relaxation of the surrounding Si host network is calculated for every location of the impurity or defect. Hellman-Feynman forces are not obtained in the present calculations. Instead, we relax the first-neighbor shell of atoms to at least three different positions, and use the resulting total energies to fit a parabola to obtain the minimum-energy distance. All relaxations reported in this work are radially away (or towards) the defect and hence are symmetry preserving. Tests have indicated that other relaxations have only minor effects on the total energy. For configurations which cause little distortion of the network (e.g., H or T), only the first shell of neighbors is relaxed. For configurations which cause severe disruption (e.g., BC), two shells of neighbors are relaxed.

In order to test all elements of this methodology, we have calculated the relaxation of the Si host surrounding neutral substitutional impurities. The four Si neighbors of substitutional B, which has a covalent radius $\approx 75\%$ that of Si,[27] experience an inward "breathing"-mode relaxation of 0.2 Å, with an accompanying decrease of the total energy of 0.8 eV. Despite its small size with respect to Si and its tendency of form threefold-coordinated molecules, B remains at the nominal substitutional site (to within 0.1 Å). Substitutional P, with a covalent radius slightly smaller than Si, is found to cause no distortion of the host network. Both As and Sb have larger covalent radii than Si and cause an outward "breathing"-mode distortion of the four neighboring Si atoms. The Si-As interatomic distance is calculated to be 2.43 Å and the Si-Sb interatomic distance is 2.54 Å. The Si-As distance is in excellent agreement with extended x-ray-absorption fine-structure (EXAFS) measurements,[28] which give 2.41 Å. The results for P and As are also in good agreement with previous total-energy calculations on positively charged substitutional donors.[29]

We estimate our total error to be less than 1 eV, depending, of course, upon the atomic configuration and the particular impurity. The majority of the error comes from the LDA uncertainty in the defect- and impurity-related levels in the energy gap. Overall, this scheme has a proven reliability in calculating bulk properties of semiconductors, reconstruction of semiconductor surfaces, and general properties of defects.[21]

III. EQUILIBRIUM DIFFUSION

A. Background and atomistic mechanisms

Under either equilibrium or nonequilibrium conditions, the diffusion coefficient D is given by a sum of contributions of the form

$$D_i = \frac{C_i d_i}{C_X} , \tag{1}$$

where C_i is the concentration of the defect i whose long-range migration effects diffusion of the substitutional dopant, d_i is the corresponding diffusivity, and C_X is the total concentration of impurities.

For the CE mechanism, the pertinent defect is the substitutional impurity itself, whereas for defect-mediated diffusion this species needs to be identified. For impurity diffusion mediated by vacancies, it is convenient to identify two distinct limits. In the first limit, impurity-vacancy binding is weak, so that when a vacancy positions itself next to an impurity, the two switch places, the vacancy migrates away, and the impurity awaits the arrival of another vacancy in order to migrate another step. Such a process is the same as that for self-diffusion; i.e., the Si vacancy is the relevant diffusing species. The impurity diffusion activation energy is equal to the sum of the vacancy-formation energy and the migration energy of either a Si atom or an impurity atom into a vacant adjacent

site, whichever is larger. Thus, the impurity diffusion activation energy for this mechanism is equal to or larger than the activation energy of self-diffusion. In the second limit, impurity-vacancy binding is strong, so that when a vacancy positions itself next to an impurity atom, migration of the *pair* occurs. After exchanging positions, the vacancy moves away from the dopant atom around a six-fold ring to at least a third-neighbor position. It can then return by a different path, placing itself next to the impurity. The vacancy and the impurity exchange and the process repeats itself. The net activation energy is the sum of the pair-formation and migration energies and can be less than the activation energy for self-diffusion.

Self-interstitial-mediated diffusion can occur in a variety of ways. Two processes believed important are what we call "coordinated push" of a self-interstitial on a substitutional impurity along the bonding direction towards a Si neighbor[13] [see Figs. 2(a)–2(c)] and the kick-out mechanism[13] [see Figs 2(d)–2(f)]. The coordinated push mechanism, similar to the vacancy-mediated mechanisms described above, has two extreme limits, depending upon the binding energy of the impurity–self-interstitial pair. In either extreme limit, at the saddle point of the coordinated push process [Fig. 2(b)] the impurity atom is at the BC site, while the neighboring Si atom is pushed off its substitutional site towards the channel T site. The impurity ends up in the next substitutional site, its former Si neighbor now in the channel as a self-interstitial [Fig. 2(c)]. The original self-interstitial is a nearest neighbor of the impurity. In the weak-binding limit, the new self-interstitial can readily migrate away and, to move to the next substitutional site, the impurity must await the arrival of another self-interstitial. In this limit, then, it is the self-interstitial which mediates long-range migration of the substitutional impurity. The activation energy for diffusion is the sum of the formation energy of the substitutional impurity–self-interstitial pair plus the migration energy of the impurity over the BC saddle point. The activation energy may thus be equal to or larger than the activation energy for self-diffusion, depending upon the differences in migration energy. In the strong-binding limit, the new self-interstitial remains bound to the substitutional impurity and the former can then execute exactly the same coordinated push. In the strong-binding limit, it is the self-interstitial–impurity *pair* which effects long-range migration of the impurity. The activation energy for the strong-binding limit may be less than the activation energy for self-diffusion as a result of binding. The second interstitial process involves the kick-out of the substitutional impurity [Fig. 2(e)] into the low-electron-density channel in which it migrates with a rather small barrier. After migration along the channel, the impurity kicks back into a substitutional site, ejecting a Si atom into the channel. The diffusing species is thus the interstitial impurity.

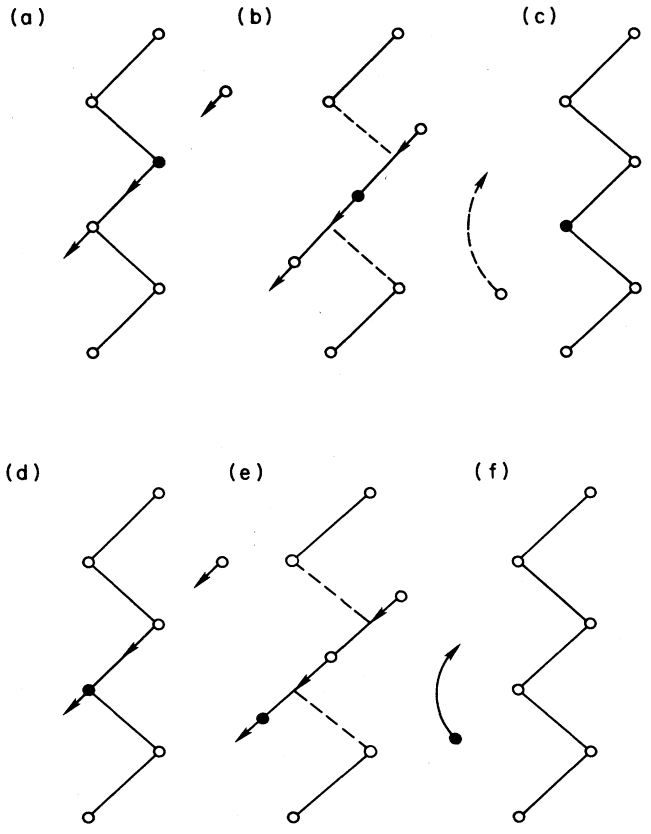

FIG. 2. Schematic diagram showing two interstitial-mediated diffusion processes considered in this paper. (a)–(c) Schematic diagram of the (110) plane in diamond structure Si depicting the "coordinated push" diffusion process. Panel (a) depicts the initial positions of all atoms, while panel (c) depicts the final positions. Panel (b) shows the saddle-point configuration. (d)–(f) The same crystal plane in Si, but now depicting the kick-out diffusion process. Panel (d) depicts the initial atomic positions, while panel (f) shows the final positions. Panel (b) depicts the saddle-point configuration.

For all mechanisms, under equilibrium conditions, the individual diffusion coefficients D_i can also be written in the Arrhenius form

$$D_i^* = D_{i,0}^* \exp(-Q_i^*/k_B T) \ . \tag{2}$$

The preexponential $D_{i,0}^*$ contains a variety of factors, including the entropy of diffusion. Q_i^* is the activation energy, k_B is Boltzmann's constant, and T is the temperature. The asterisks denote equilibrium quantities. For the CE mechanism, Q_i^* is the energy required to place an impurity atom and one of its Si neighbors at the exchange-path saddle point. For defect-mediated mechanisms, Q_i^* is the sum of the formation and migration energies for the diffusing species.

The determination of Q_i^* for the CE mechanism necessitates mapping out the entire exchange path and identifying the lowest-energy saddle point. Pandey[14] has carried out such a task in the case of self-diffusion (Si-Si exchange), but the reoptimization of the entire impurity-Si exchange is an unduly demanding computational exercise. For our purposes, it was adequate to obtain an upper bound for the saddle-point energy. We assumed the same path as for the Si-Si exchange, calculated the to-

tal energy of the saddle point, and included the relaxation of the neighboring atoms by using Pandey's calculated relaxation for pure Si (0.75 eV).

In general, for defect-mediated diffusion, the defects responsible for diffusion may exist in several charge states, each of which can contribute to diffusion. For the temperatures at which diffusion experiments are performed (900–1100 °C), even for relatively high doping levels (e.g., $10^{18}-10^{19}$ cm^{-3}), the Fermi level is at midgap. Previous calculations[13] on dopants in Si have shown that all charge states have roughly the same formation energies for interstitial impurities or impurity-vacancy pairs when the Fermi level is near midgap (to within approximately 0.3 eV). The energetics of diffusion are therefore relatively insensitive to the dopant charge state. In this paper, we report results for neutral species only.

Formation energies for any impurity-defect complex are always defined in our calculations with respect to the substitutional impurity in the absence of any defects. The formation energy for an impurity-vacancy pair (XV) in an N-atom cell is defined as

$$E_f(XV) \equiv E(XV) - E(X_s) + \frac{1}{N} E_{\text{bulk}} , \tag{3}$$

where $E(XV)$ is the calculated total energy per supercell containing an impurity-vacancy pair, $E(X_s)$ is the total energy per supercell containing a substitutional impurity, and E_{bulk} is the total energy per supercell of pure bulk Si. The formation energy for an interstitial impurity (X_i) in an N-atom cell is defined as

$$E_f(X_i) \equiv E_f(I) + [E(X_i) - E(X_s\text{-}I)] , \tag{4}$$

where $E_f(I)$ is the formation energy of a Si self-interstitial, $E(X_i)$ is the total energy per supercell containing an interstitial impurity, and $E(X_s\text{-}I)$ is the total energy per supercell containing a (substitutional impurity–I) pair. The formation energy of an I in pure Si is defined as

$$E_f(I) \equiv E(I) - \frac{N+1}{N} E_{\text{bulk}} , \tag{5}$$

where $E(I)$ is the total energy per supercell containing a Si interstitial. Note that it makes no difference in finding the formation energy of an interstitial impurity which position we use for the Si interstitial, as long as we use a consistent choice throughout Eq. (4). Note also in Eq. (4) that the second term is just the energy of exchanging an interstitial Si and a substitutional impurity.

For defect-mediated pathways, the first task of theory is to determine which defect or complex leads to diffusion with the smallest Q_i^*. For all impurities, the formation energies of the impurity-vacancy complexes are calculated with appropriate relaxations, etc. However, because a supercell beyond present computer capacity is required to obtain the migration energy, we have taken these values from experiment (for P, As, and Sb) (Ref. 30) or used a simple estimate (for B). See Table I for the actual values used. For vacancy-mediated (V-mediated) B diffusion, we find that there is a relatively small binding energy between the impurity and the defect, where the binding energy of an impurity-defect complex is defined as the difference between the formation energy of the defect in pure Si and the formation energy of the impurity-defect complex (see Table I). In particular, we note that the binding energy of the BV pair is smaller than our estimated migration energy. Given the error bars of our calculation, we cannot discern between a simple vacancy mechanism or a BV-pair mechanism. For all other impurities, however, the relevant diffusing species is the impurity-vacancy pair.

For interstitial-mediated pathways, a global total-energy surface depicting the interactions between N Si atoms and a single impurity in an N-atom supercell was

TABLE I. Calculated activation energies (Q^*) under equilibrium conditions for B, P, As, and Sb diffusion as well as Si self-diffusion. Listed also are the separate contributions to Q^* and the binding energies (E_b) of impurity-vacancy pairs. All quantities are in eV and all species are in their neutral charge state. The experimental binding energies are from Ref. 15 and the Si CE value is from Ref. 14.

Species	Q^*	E_f	E_m	E_b(theor)	E_b(expt)
B_i	3.9	3.9	0.0		
BV	a	3.0	1.0	0.5	
B(CE)	4.9				
P_i	3.8	3.0	0.8		
PV	3.4	2.5	0.94	1.0	1.04
P(CE)	4.6				
As_i	3.6	3.2	0.4		
AsV	3.4	2.3	1.07	1.2	1.23
As(CE)	3.9				
Sb_i	4.9	4.7	0.2		
SbV	3.6	2.3	1.28	1.2	1.44
Sb(CE)	4.5				
Si_i	4.0	3.6	0.4		
SiV	3.8	3.5	0.3		
Si(CE)	4.3				

[a]Since $E_m > E_b$, the BV pair is not a stable diffusing species. See the text for further explanation.

required in order to ascertain the lowest-energy diffusion pathways and the migrating species. Such a surface results from the collection of the total energies of $N+1$ atoms competing for N substitutional sites with the relaxation of the surrounding host crystal included for each configuration. The details of generating a total-energy surface are described elsewhere.[22] Because the total-energy surface is a function which depends upon the three spatial dimensions, it is easiest to examine a slice through a given crystal plane. The energy surface can be displayed either as a contour plot (the contours depicting constant energies) or as a perspective plot (the in-plane coordinates are the chosen diamond-structure coordinates and the third axis is the energy). We emphasize that for either type of plot, the relaxation of the host crystal is included in obtaining the total energy, but the positions marked as atoms serve only as a template for identifying positions in the crystal plane.

A contour plot of the total-energy surface depicting the diffusion of a neutral B atom through the diamond-structure (110) plane is shown in Fig. 3(a). A perspective plot for the same species is shown in Fig. 3(b). In constructing both figures, the zero of energy was chosen at the saddle point of the B kick-out process [see Fig. 3(a) and below]. In the perspective plot, regions of different energy have been color-coded: the lowest-energy regions are red, follow by blue, with the highest-energy regions in green. The lowest-energy migration pathway for neutral B is along the low-electron-density channels; indeed, there is virtually no barrier to migration from the H to the T site, etc. If, instead of moving along the channel, the B atom continues in a $\langle 111 \rangle$ direction towards a substitutional Si atom, a kick-in process is initiated. The impurity climbs up energy contours in the direction of the saddle point. The saddle point for this process is roughly two-thirds of the way from the T site to the substitutional site. Although it is not shown in Figs. 3(a) and 3(b), the relaxation of the two Si atoms along the [111] direction ahead of the B atom is accounted for in constructing the total-energy surface, as are relaxations of the second neighbors. The energy barrier to the kick-in process via this pathway is ≈ 1 eV. Once the B atom has passed the kick-in saddle point, its energy decreases towards the substitutional site, while the furthest Si atom is kicked out into the channel. The reverse of the kick-in process depicted in the total-energy surfaces is the kick-out process, and it represents the lowest-energy mechanism by which substitutional B becomes an interstitial. In sum, the diffusing species is thus the interstitial B atom. We find qualitatively similar results for all dopants studied; the diffusing species for interstitial-mediated pathways is always the interstitial impurity which is created by the kick-out process.

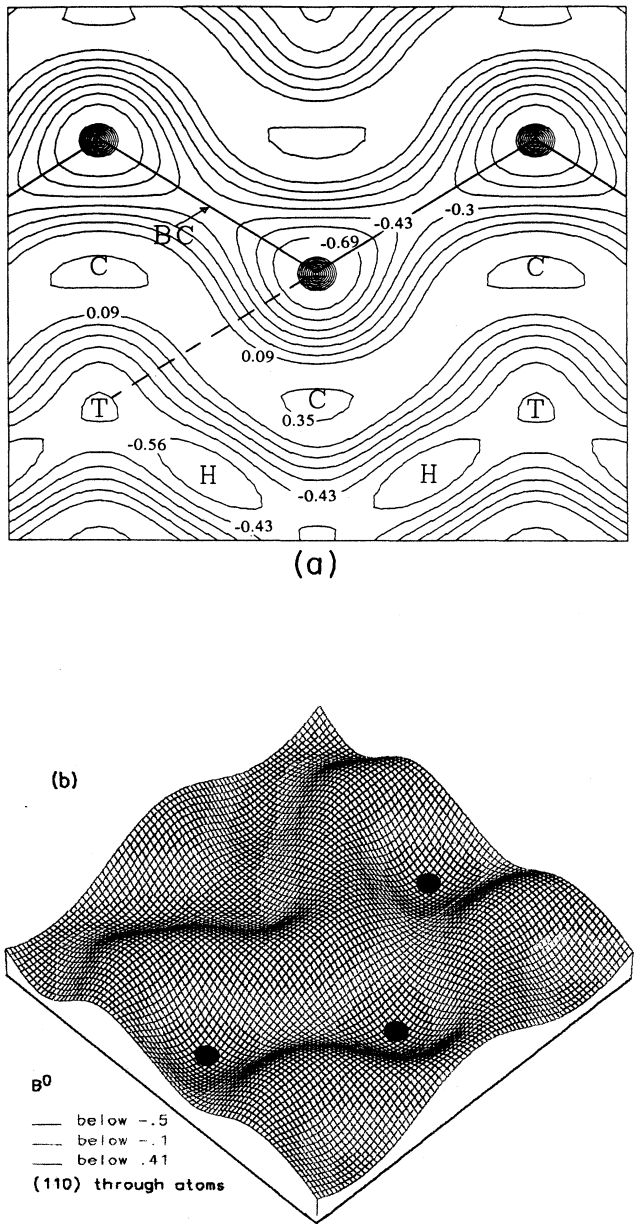

FIG. 3. Total-energy surface plots. (a) Total-energy contour plot depicting the migration of a neutral B interstitial through the Si crystal. The labeled sites are T (tetrahedral), H (hexagonal), BC (bond-center) and C (at the center of a rhombus formed by three adjacent Si atoms and the nearest T). The energy difference between contours is 0.13 eV. The dashed line is the kick-out pathway. The values of the contours near the channel regions are ≈ 0.2 eV higher than those reported in our previous publication (Ref. 16). This is a consequence of generating the surface with a higher plane-wave cutoff and does not change any of our conclusions based on that previous figure. (b) Perspective plot of the same process. The areas colored red are lowest in energy, blue are intermediate, followed by the highest-energy regions in green. Relaxations of the host atoms are not indicated in the figure, but are taken into account in the total-energy calculations.

B. Results and discussion

The calculated activation energies for CE-, V-, and I-mediated mechanisms for substitutional B, P, As, and Sb diffusion under equilibrium conditions are shown graphically in Fig. 4. A selected range of experimental values is shown as boxed areas in Fig. 4 as well. Actual values for

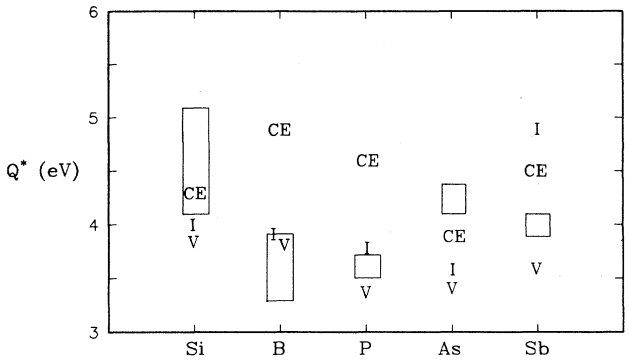

FIG. 4. The calculated activation energies under equilibrium conditions for vacancy-mediated (V), interstitial-mediated (I), and concerted exchange (CE) mechanisms for Si self-diffusion and various impurities. The boxed areas are a selected range of experimental results from Ref. 20.

Q_i^* and the contributions to it are given in Table I. For comparison, the calculated values for Si self-diffusion are also shown (the CE value is that reported in Ref. 14). The calculated values presented in Fig. 4 and Table I for interstitial-mediated diffusion are those for *impurity* interstitial diffusion, effected by the kick-out mechanism. Calculated activation energies for both extreme binding limits of the coordinated push mechanism are significantly larger than the activation energies for the kick-out mechanism, thereby ruling out the impurity–self-interstitial pair and the self-interstitial as the relevant diffusing species. For B, P, and As, the differences between V- and I-type mechanisms are smaller than our estimated error bar (0.4 eV is the maximum difference). Furthermore, because the CE activation energies are upper bounds, we view them as comparable to defect-assisted pathways. Only for Sb impurities is one mechanism dominant: the V-assisted pathway is a full 1.3 eV lower than the I-assisted pathway, so that the vacancy mechanism prevails, in agreement with conclusions drawn from experimental data.[8]

From our calculations we can also obtain the binding energies of the various impurity-vacancy complexes. The binding energies of some impurity-vacancy pairs have been measured experimentally[15] and are included in Table I along with the theoretical values. We note for P, As, and Sb that the impurity-vacancy binding energies are slightly larger than the pair-migration energies, suggesting that it is at least energetically feasible for such complexes to migrate. None of these impurities is in the strong-binding limit and we therefore consider the range of activation energies between the simple vacancy mechanism and the impurity-vacancy pair as the error bar for the vacancy-mediated process.[31] However, as pointed out in the preceding subsection, the binding energy of BV pairs is rather small (0.5 eV smaller than our estimated migration energy), so that if B diffuses by a vacancy mechanism, it is probably effected by the isolated vacancy, as opposed to the pair mechanism. We discuss this point more fully in the next section. The relative magnitudes of the binding and migration energies also have important consequences for the electrical deactivation of heavily doped Si.[32]

In summary, our calculated equilibrium activation energies, being in the same range as experimental values, establish the reliability of our calculational approach, but do not establish the relative importance of the various mechanisms, with the exception of Sb. In order to do this within the confines of equilibrium diffusion, calculations of the various preexponentials are required. Reliable entropy calculations are not currently possible, however. Nonetheless, we will demonstrate in the remainder of this paper that, within a suitable framework for nonequilibrium diffusion, theoretical calculations of various barrier heights, etc., combined with experiments involving injection of excess point defects, do allow a number of definitive conclusions to be drawn.

IV. NONEQUILIBRIUM DIFFUSION

A. Theory of externally stimulated diffusion

Under equilibrium conditions, the point defects responsible for diffusion are created thermally. However, evidence has accumulated that surface treatments selectively inject point defects into the bulk. Oxidation, for example, injects self-interstitials, while direct nitridation injects vacancies.[5] Under injection conditions, the dopant diffusion coefficient has been observed to be either enhanced or retarded. Such experiments have, however, led to widely conflicting conclusions regarding the dominant diffusion mechanism, largely because of contradictory assumptions. Virtually all attempts at constructing a theory for diffusion under point-defect injection have relied on unclear postulates, mainly with regard to the relevant diffusing species. Most theories assume that the concentrations of vacancies and self-interstitials determine the dopant diffusion coefficient. A review and critique of the early work may be found in Ref. 6. As we showed in Sec. III of the present paper, for P, As, and Sb, it is certainly true that the relevant diffusing species are either the interstitial impurity or the impurity-vacancy pair. For B, the interstitial impurity, the isolated vacancy, or the impurity-vacancy pair may control long-range dopant migration.

A correct theory of nonequilibrium diffusion rests upon the realization that the diffusion coefficient D is still given by a sum of expressions of the form of Eq. (1) with the individual diffusivities the same as under equilibrium. The task, then, of such a theory is to determine the relevant species concentrations, taking account of their creation, annihilation, and interaction with the other species present. In this subsection, we present the details of such a theory under self-interstitial injection (the case for vacancy injection is entirely analogous). In the second part of this subsection, these results are combined with experimental results to assess the contribution of the various mechanisms to the diffusion of dopant impurities.

Nonequilibrium dopant diffusion experiments provide a convenient framework within which the contribution of the CE mechanism can be investigated. The CE diffusion

coefficient is proportional to the fraction of impurities that are substitutional, C_{X_s}. Thus, point-defect injection can only affect the CE mechanism through changes in C_{X_s}; e.g., through formation of impurity-vacancy pairs or interstitial impurities. However, injection occurs at low levels relative to C_{X_s}, so that it affects C_{X_s} and hence D_{CE} only minimally. Therefore, if the CE is the dominant mechanism, the diffusion coefficient should be either unchanged, or, if the injection process is efficient, so that diffusion may proceed by a vacancy- or interstitial-mediated mechanism, then *enhanced* diffusion should be observed. Under no circumstances should diffusion be retarded by moderate rates of injection. This is in contradiction to the experimental observation that B, P, As, and Sb all show significant retardation under one or another defect-species injection.[7,8] The CE mechanism therefore cannot be the dominant impurity diffusion mechanism and we do not discuss it any further in the following.

The task remaining is thus to determine the effects of point-defect injection on point-defect-mediated diffusion. This is accomplished by finding the concentrations of the relevant diffusing species which may be the impurity interstitial, the impurity-vacancy pair, or, for the case of B, the Si vacancy. The concentrations of all species are governed by the following *complete* set of reactions:

$$S \rightleftarrows V \ , \tag{6}$$

$$S \rightleftarrows I \ , \tag{7}$$

$$I + X_s \underset{k_1'}{\overset{k_1}{\rightleftarrows}} X_i \ , \tag{8}$$

$$V + X_s \underset{k_2'}{\overset{k_2}{\rightleftarrows}} XV \ , \tag{9}$$

$$I + XV \underset{k_3'}{\overset{k_3}{\rightleftarrows}} X_s \ , \tag{10}$$

$$V + X_i \underset{k_4'}{\overset{k_4}{\rightleftarrows}} X_s \ , \tag{11}$$

$$I + V \underset{k_5'}{\overset{k_5}{\rightleftarrows}} \square \ . \tag{12}$$

Reactions (6) and (7) are schematic and represent the independent thermal generation or annihilation of interstitials or vacancies by free or internal surfaces, S. Rate constants for the various reactions are denoted k_1, k_1', etc. In Eq. (12), $\square$ represents bulk Si. From first-principles calculations,[33] we have found significant barriers for the reverse reactions (10)–(12), indicating that the bulk plays only a small role in supplying point defects.

Following experimental measurements of the dopant diffusion coefficient under point-defect injection, we distinguish two time domains. All data to date show on the time scale of $\lesssim 1$ hour nonconstant diffusion coefficients: D is initially equal to the equilibrium value, attains an extremum value, and finally decreases or increases to some final steady-state value. During the transient period, under injection of either vacancies or self-interstitials, *all* impurities are expected to show enhanced diffusion. This phenomenon is a consequence of the increased concentration of I or V which, because the concentration of X_s is many orders of magnitude larger than that of XV or X_i, drives Eqs. (8) or (9), respectively, further to the right, increasing the concentration of the diffusing species. In addition, we have calculated a barrier of ≈ 1 eV for I-V recombination,[33] indicating that the point defects do not readily recombine. Observation of the initial transient behavior initially led Antoniadis and Moskowitz[7] to suggest the existence of such a recombination barrier. From their data, they estimate a barrier of ≈ 1.4 eV. Enhanced diffusion is observed experimentally[8] for B, P, As, and Sb under interstitial injection, and for As and Sb under vacancy injection on the short-time scale. P under vacancy injection does, however, show consistently retarded diffusion for all times measured. It is not clear why this should be the case.

We now turn to consideration of the diffusion problem under point-defect injection at steady state. From the seven reactions listed above [Eqs. (6)–(12)], four expressions for the time rate of change of the concentrations of I, V, XV, and X_i may be readily obtained:

$$\frac{\partial C_I}{\partial t} = g_{\mathrm{th}}^I - r_{\mathrm{th}}^I C_I + g_{\mathrm{inj}} - k_1 C_I C_{X_s} + k_1' C_{X_i} - k_3 C_I C_{XV} + k_3' C_{X_s} - k_5 C_I C_V + k_5' C_{\mathrm{Si}} = 0 \ , \tag{13}$$

$$\frac{\partial C_V}{\partial t} = g_{\mathrm{th}}^V - r_{\mathrm{th}}^V C_V - k_2 C_V C_{X_s} + k_2' C_{XV} - k_4 C_V C_{X_i} + k_4' C_{X_s} - k_5 C_I C_V + k_5' C_{\mathrm{Si}} = 0 \ , \tag{14}$$

$$\frac{\partial C_{XV}}{\partial t} = k_2 C_V C_{X_s} - k_2' C_{XV} - k_3 C_I C_{XV} + k_3' C_{X_s} = 0 \ , \tag{15}$$

$$\frac{\partial C_{X_i}}{\partial t} = k_1 C_I C_{X_s} - k_1' C_{X_i} - k_4 C_V C_{X_i} + k_4' C_{X_s} = 0 \ , \tag{16}$$

where g_{th}^I (g_{th}^V) is a thermal surface generation rate for I (V), r_{th}^I (r_{th}^V) is a thermal surface recombination frequency for I (V), g_{inj} is the surface injection rate for interstitials, C_{Si} is the concentration of Si lattice sites, and all other terms are as defined above. We have excluded any spatial dependence in the concentrations for reasons of simplification. This amounts to assuming that the impurity profile is flat in the region of interest. The resulting set of four equations is a complete and exact set, which can, in principle, be solved for all the relevant concentrations. This result is singular and contrasts strikingly with previous work wherein differing sets of equations were written down which were either incomplete or taken as self-evident.[6]

In practice, a series of approximations are required be-

fore analytical results can be obtained. For each species, the dominant generation and recombination term or terms are identified and are then used to solve for the concentrations. The general guiding principle in determining the dominant terms is based on a knowledge of the relative barrier heights as found from our first-principles calculations. For example, our calculations show that bulk generation of I and V defects through Frenkel-pair formation requires at least 8 eV, making this an unlikely source of either point defect. We extend this result to the reverse of reactions (10) and (11). Furthermore, because the binding energies of XV or X_s-I pairs are relatively small (≈ 1 eV, see Table I), we assume that Eqs. (8) and (9) are in local equilibrium. Finally, for the case of self-interstitial injection, the annihilation of X_i by vacancies (the minority species) is likely to be a second-order effect, and thus we ignore it.

From these general considerations, the point-defect concentrations are

$$C_I = \frac{g_{\rm th}^I + g_{\rm inj}}{r_{\rm th}^I} = C_I^* + C_I' \ , \tag{17}$$

$$\frac{1}{C_V} = \frac{r_{\rm th}^V + k_5 C_I}{g_{\rm th}^V} = \frac{1}{C_V^*} + \frac{k_5 (C_I^* + C_I')}{g_{\rm th}^V} \ . \tag{18}$$

The asterisks denote equilibrium quantities, while the primes denote just that component due to the nonequilibrium process. We note in passing that the often-quoted relationship

$$C_I^* C_V^* = C_I C_V \tag{19}$$

used in the analysis of injection experiments *does not hold* for the general case under consideration here. Hu has discussed the shortcomings and fallacies associated with the assumption of Eq. (19) more extensively, and we refer the interested reader to that article.[6]

Using Eqs. (17) and (18), and the general considerations outlined above for choosing the dominant terms for generation and recombination, we find, for the nonequilibrium concentrations of C_{X_i} and C_{XV},

$$C_{X_i} = C_{X_i}^* + \frac{k_1 C_{X_s} C_I'}{k_1'} \ , \tag{20}$$

$$\frac{1}{C_{XV}} = \left[1 + \frac{k_5 (C_I^* + C_I')}{r_{\rm th}^V} \right] \left[\frac{1}{C_{XV}^*} + \frac{k_3 C_I'}{k_2 C_{X_s} C_V^*} \right] \ . \tag{21}$$

The species whose concentration is enhanced by interstitial injection, C_I or C_{X_i}, exhibit a simple additive dependence on the injected species. On the other hand, the species which may be annihilated by interstitial injection, C_V or C_{XV}, show an inverse dependence on the interstitial concentration. We will return to this point later.

Combining Eqs. (1), (20), and (21), the total diffusion coefficient is of the form

$$D = D_I + D_V \ , \tag{22}$$

where

$$D_I = D_I^* + D_I' \tag{23}$$

and

$$\frac{1}{D_V} = \frac{1}{D_V^*} + \frac{1}{D_V'} \ , \tag{24}$$

where the subscript I (V) denotes the I- (V-) assisted component of diffusion. In principle, each component may consist of several terms. For example, B diffusion assisted by vacancies may be mediated by either the isolated vacancy, the B-V pair, or by both. However, for all other impurities studied here, the I- or V-assisted mechanism is mediated by a single species.

Activation energies for the nonequilibrium part of diffusion may be obtained by combining Eqs. (1) and (2) with the relevant species concentration. The latter quantity is expressed in terms of the various barrier heights, etc. Specifically, D_I' is activated with an activation energy

$$Q_I' = E_{\rm inj} - \Delta E + E_m \ , \tag{25}$$

where $E_{\rm inj}$ is the activation energy of the interstitial injection process, ΔE is the energy difference between X_i and X_s-I as in reaction (8), and E_m is the migration energy of X_i. The first term follows from experiments performed by Hu[5] in which it was observed that interstitial injection results in the growth of stacking faults and that this process is activated. We infer that the interstitial injection process is itself also activated and therefore the I concentration is given by

$$C_I' \propto e^{-E_{\rm inj}/k_B T} \ . \tag{26}$$

The second term follows from

$$\frac{k_1}{k_1'} \propto e^{\Delta E/k_B T} \ . \tag{27}$$

In the limit that the vacancy concentration is unperturbed from its equilibrium value, then Eq. (21) may be simplified to

$$\frac{1}{C_{XV}} = \frac{1}{C_{XV}^*} + \frac{k_3 C_I'}{k_2 C_{X_s} C_V^*} \ . \tag{21'}$$

From Eq. (21'), D_V' is activated with an activation energy

$$Q_V' = (E_{\rm inj} + E_{I\text{-}XV}^{\rm barrier}) - (E_f^V + E_{V\text{-}X_s}^{\rm barrier}) + E_m \ , \tag{28}$$

where $E_{I\text{-}XV}^{\rm barrier}$ ($E_{V\text{-}X_s}^{\rm barrier}$) is the energy barrier to recombination of interstitials (vacancies) with XV pairs (X_s), E_f^V is the thermal formation energy of vacancies, and E_m is the XV migration energy. The various terms in the activation energy arise as above or from the following expressions:

$$k_3 \propto e^{E_{I\text{-}XV}^{\rm barrier}/k_B T} \ , \tag{29}$$

$$k_2 \propto e^{E_{V\text{-}X_s}^{\rm barrier}/k_B T} \ , \tag{30}$$

and

$$C_V^* \propto e^{E_f^V/k_B T} \ . \tag{31}$$

Equation (28) has a simple physical interpretation. The first term in parentheses is the energy required to annihilate the diffusing XV pairs, while the second term represents the energy required to produce the pairs initially. The overall activation energy is the competing cost of these two terms, in addition to the migration energy.

Diffusion coefficients measured under point-defect injection at several temperatures may appear misleadingly complex. From Eqs. (23) and (24), both diffusion coefficients can display non-Arrhenius behavior which obscures determination of an activation energy. To extract meaningful information from temperature-dependent data, it is necessary to isolate the equilibrium and nonequilibrium contributions to the total diffusion coefficient. If diffusion is mediated by self-interstitials, then under interstitial injection the nonequilibrium diffusion coefficient (D_I') is obtained by subtracting the (known) equilibrium diffusion coefficient (D_I^*) from the total diffusion coefficient (D_I). The two possible resulting forms for D_I' are shown schematically in Figs. 5(a) and 5(b). Such figures, which assume Arrhenius behavior for the nonequilibrium diffusion contribution, clearly assume only one species contributes to interstitial-mediated diffusion.

On the other hand, if diffusion is mediated by vacancies, then under interstitial injection the diffusion coefficient displays an inverse behavior [Eq. (24)]. This dependence naturally suggests introducing an *inverse* Arrhenius plot of $1/D_V$ versus $1/T$. The nonequilibrium diffusion coefficient (D_V') is thus determined from rearranging Eq. (24),

$$\frac{1}{D_V'} = \frac{1}{D_V} - \frac{1}{D_V^*} \,. \tag{24'}$$

The two possible forms for measured diffusion coefficients are shown in Figs. 6(a) and 6(b). From any of these four plots, Figs. 5(a), 5(b), 6(a), and 6(b), the contribution due solely to the nonequilibrium process can be isolated and, hence, a corresponding activation energy that can be compared to either Eq. (25) or (28) may be found.

B. Results and discussion

We now turn to a discussion of three distinct cases. Consider the instance in which, under equilibrium, the I

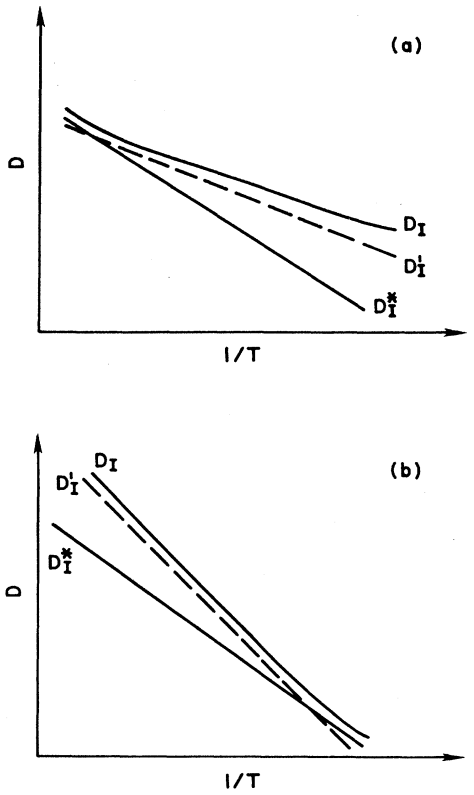

FIG. 5. (a) and (b) Arrhenius plot for interstitial-mediated diffusion under interstitial injection. D_I^* denotes the equilibrium diffusion coefficient, D_I the total diffusion coefficient under nonequilibrium conditions, and the dashed line is the nonequilibrium contribution (D_I')

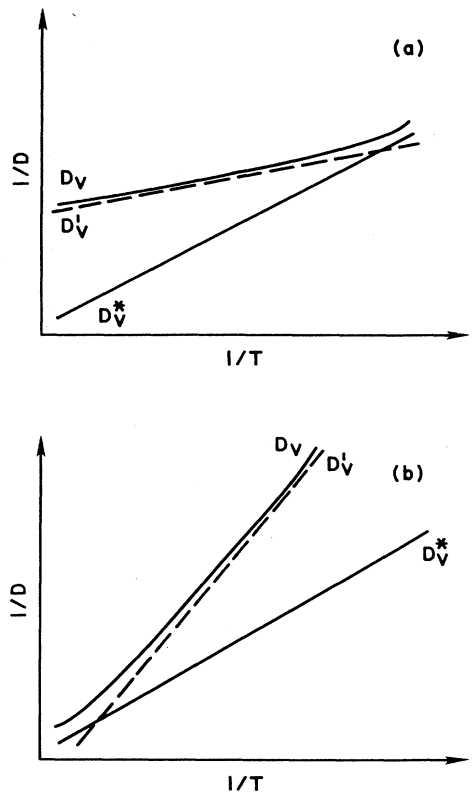

FIG. 6. (a) and (b) Reciprocal Arrhenius plot for vacancy-mediated diffusion under interstitial injection. D_V^* denotes the equilibrium diffusion coefficient, D_V the total diffusion coefficient under nonequilibrium conditions, and the dashed line is the nonequilibrium contribution (D_V').

TABLE II. Activation energies (Q') for diffusion mediated exclusively by interstitials under interstitial injection (theory) and measured activation energies under oxidation conditions (experiment from Hill, Ref. 34). All quantities are in eV.

Species	Q'(theor)	Q'(expt)
B	2.6	2.3
P	2.5	2.4
As	2.3	2.3

component is dominant. Interstitial injection leads to enhanced diffusion of the form

$$D = D^* + D' , \tag{32}$$

where the activation energy of D' is as given in Eq. (25). The measured diffusion coefficient may have either of the forms depicted in Fig. 5(a) or 5(b). Hill[34] has measured the diffusion coefficients of B, P, and As under interstitial injection and found that they indeed obey Eq. (32) and are similar to that depicted in Fig. 5(a). This observation suggests therefore that these impurities diffuse principally by an interstitial mechanism. In order to further test this possibility, we have calculated the activation energy for these impurities under interstitial injection [Eq. (25)] using our calculated values for ΔE and E_m and a value for the interstitial injection energy, E_{inj}, extracted from the data of Ref. 35. These results, along with Hill's experimental values, are given in Table II. The excellent agreement between the two sets of values corroborates the conclusion that these impurities diffuse primarily assisted by interstitials.

Using a damaged layer created by Ar-ion implantation as the interstitial source, Bronner and Plummer[36] observed P diffusion enhancement over a limited temperature range. They measured a dependence for the diffusion coefficient very similar to Fig. 5(a), as was found by Hill, but did not take data at temperatures high enough to discern any curvature in the Arrhenius plot. Furthermore, they did not determine E_{inj}. But, using their measured activation energy for the total diffusion coefficient, 1.3 eV, we may infer a value for E_{inj}. Because the total diffusion-coefficient curve and the nonequilibrium contribution to it are essentially parallel over the limited temperature range investigated, solving Eq. (25) for E_{inj} and inserting our theoretical values, we find $E_{\text{inj}} = 1.1$ eV, a value which can be tested experimentally.

We noted in the preceding subsection on equilibrium diffusion that the BV pair has a rather small binding energy compared to its migration energy. This means that it is more likely that the isolated vacancy, rather than the pair, effects long-range migration of B, if indeed a vacancy mechanism is appropriate. In turn, then, the diffusion coefficient of B is determined not by the BV concentration, but by the isolated V concentration [Eq. (18)]. Under interstitial injection, the isolated vacancy concentration is less than or equal to the equilibrium concentration, so that either no change in the diffusion coefficient is observed or diffusion is retarded. This is clearly in contradiction to Hill's experiments, which show enhancement. We cite this finding as further proof that B migration is mediated predominantly by Si self-interstitials.

If equilibrium diffusion is mediated primarily by vacancies, interstitial injection can lead to either enhanced or retarded diffusion depending upon the level of injection. At low injection levels, which may be achieved by oxidation at moderate temperatures, the majority V component is retarded according to Eq. (24), while the I component remains small, with a diffusion coefficient given by Eq. (23). There are a number of data which support the contention that Sb diffusion does indeed exhibit retardation under interstitial injection.[8] Based on the theory presented in the preceding subsection, we predict that temperature-dependent data would obey Eq. (24), so that a reciprocal Arrhenius plot would be required in order to find an activation energy for D'_V to be compared with Eq. (28). The measured diffusion coefficient under such conditions would have a form schematically similar to either Fig. 6(a) or 6(b). Such experiments, which have not been performed to date, would provide a test of our theory and furnish a basis by which the conclusion that Sb diffusion is vacancy dominated can be assessed. At high interstitial injection levels, the interstitial contribution will ultimately overwhelm all other terms, and enhanced diffusion with an activation energy given by Eq. (25) would be observed. However, data are usually reported at a single temperature, so that no crossover from retardation to enhancement has been observed.

Lastly, if both the I and V components under equilibrium conditions are comparable, plots of the diffusion coefficient under interstitial injection would be rather complex. Enhanced *or* retarded diffusion could, according to Eqs. (23) and (24), be observed. However, examining the various possible combinations of Figs. 5(a) and 5(b) with Figs. 6(a) and 6(b) yields, under certain conditions, a unique diffusion coefficient which *crosses* the corresponding equilibrium curve. This is depicted schematically in Fig. 7. Such a crossing provides a definitive experimental signature that the I and V components contribute with comparable magnitudes. Temperature-

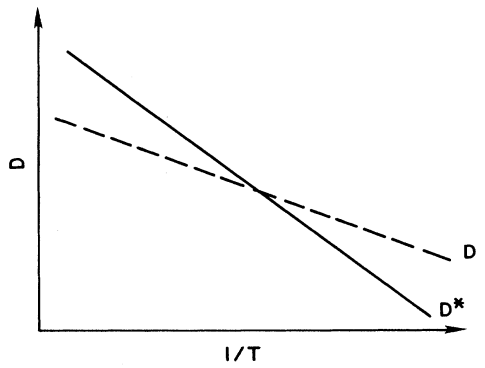

FIG. 7. Predicted schematic form for the diffusion coefficient if, under equilibrium, the I and V components are comparable.

dependent data of diffusion under point-defect injection, which may be utilized to search for this crossing, are currently not available.

V. CONCLUSIONS

In this paper we have developed a consistent framework for understanding dopant diffusion in semiconductors on a microscopic level. This framework provides important insight into the dynamics of diffusion both energetically (through expressions or calculated values for the activation energy) and pictorially (through the use of a total-energy surface). The expressions for the activation energies under various assumptions regarding the diffusion mechanism and the injected species of point defect also provide a readily accessible link between first-principles theoretical calculations and experiment.

Specifically, we conclude that B, P, and As diffusion is mediated predominantly by interstitials, whereas Sb diffusion is mediated primarily by vacancies. In large part, we confirm the conclusions of Fahey and coworkers[8] with respect to the point-defect mechanism. However, we contradict the finding of Mathiot and Pfister[7] with regard to P diffusion. The discrepancy between the two conclusions can be traced to the fact that, due to the symmetry of the relevant equations, the simulations of Mathiot and Pfister could only discern that one of the two point defects is dominant. Their choice of vacancies over interstitials was based solely on comparisons of impurity diffusion with conclusions regarding self-diffusion which exhibit the same ambiguity. In other words, the equations governing self-diffusion are symmetric with respect to the choice of vacancies or interstitials and this ambiguity propagates to the choice of a dominant defect for impurity diffusion.

The methodology presented here is by no means limited to the study of dopants in Si, but can foreseeably be applied to other impurities in semiconductors or even in metallic systems. Furthermore, the expressions developed for the activation energies can be used to probe the various external processing conditions themselves.

ACKNOWLEDGMENTS

One of us (C.S.N.) would like to acknowledge many helpful conversations with P. M. Fahey and S. M. Hu. This work was supported in part by U.S. Office of Naval Research (ONR) Contract No. N00014-84-C-0396.

---

*Present address: Philips Laboratories, 345 Scarborough Road, Briarcliff Manor, NY 10510.

[1]Fick's laws were first written down in 1855. A Fick, Pogg. Ann. **94**, 59 (1855). The first application to diffusion in solids seems to date from H. Braune, Z. Phys. Chem. **110**, 147 (1924).

[2]See, for example, *Atomic Diffusion in Semiconductors*, edited by D. Shaw (Plenum, London, 1973), for further details concerning the basic principles of diffusion.

[3]See, for example, W. Frank, U. Gösele, H. Mehrer, and A. Seeger, in *Diffusion in Crystalline Solids*, edited by G. E. Murch and A. S. Nowick (Academic, Orlando, FL, 1984), p. 63.

[4]The literature documenting the effects of surface processing conditions on the bulk point-defect concentration is extensive. See, for example, S. M. Hu, Appl. Phys. Lett. **51**, 308 (1987), and the appropriate references therein.

[5]These conclusions are based on growth or shrinkage of extrinsic stacking faults. See, for example, S. M. Hu, J. Appl. Phys. **45**, 1567 (1974); S. Mizuo, T. Kusaka, A. Shintani, M. Nanba, and H. Higuchi, *ibid.* **54**, 3860 (1983); Y. Hayafuji, K. Kajiwara, and S. Usui, *ibid.* **53**, 8639 (1982).

[6]S. M. Hu, J. Appl. Phys. **57**, 1069 (1985).

[7]D. A. Antoniadis and I. Moskowitz, J. Appl. Phys. **53**, 6788 (1982).

[8]P. Fahey, G. Barbuscia, M. Moslehi, and R. W. Dutton, Appl. Phys. Lett. **46**, 784 (1985).

[9]B. J. Mulvaney and W. B. Richardson, Appl. Phys. Lett. **51**, 1439 (1987), and references therein.

[10]F. F. Morehead and R. F. Lever, Appl. Phys. Lett. **48**, 151 (1986).

[11]D. Mathiot and J. C. Pfister, J. Appl. Phys. **55**, 3518 (1984).

[12]G. A. Baraff, M. Schlüter, and G. Allan, Phys. Rev. B **50**, 739 (1983).

[13]R. Car, P. J. Kelly, A. Oshiyama, and S. T. Pantelides, Phys. Rev. Lett. **54**, 360 (1985).

[14]K. C. Pandey, Phys. Rev. Lett. **57**, 2287 (1986).

[15]P. M. Fahey, P. B. Griffin, and J. D. Plummer, Rev. Mod. Phys. **61**, 289 (1989).

[16]C. S. Nichols, C. G. Van de Walle, and S. T. Pantelides, Phys. Rev. Lett. **62**, 1049 (1989).

[17]P. Hohenberg and W. Kohn, Phys. Rev. **136**, B864 (1964); W. Kohn and L. J. Sham, *ibid.* **140**, A1133 (1965). The exchange and correlation potentials are based on work by D. M. Ceperley and B. J. Alder, Phys. Rev. Lett. **45**, 566 (1980), as parametrized by J. Perdew and A. Zunger, Phys. Rev. B **23**, 5048 (1981).

[18]D. R. Hamann, M. Schlüter, and C. Chiang, Phys. Rev. Lett. **43**, 1494 (1979).

[19]J. Ihm, A. Zunger, and M. L. Cohen, J. Phys. C **12**, 4409 (1979).

[20]Y. Bar-Yam and J. D. Joannopoulos, Phys. Rev. B **30**, 1844 (1984).

[21]W. Pickett, Computer Phys. Rep. (to be published).

[22]C. G. Van de Walle, P. J. H. Denteneer, Y. Bar-Yam, and S. T. Pantelides, Phys. Rev. B **39**, 10 791 (1989).

[23]P. J. H. Denteneer, C. G. Van de Walle, and S. T. Pantelides, Phys. Rev. B **39**, 10 809 (1989).

[24]G. B. Bachelet, D. R. Hamann, and M. Schlüter, Phys. Rev. B **26**, 433 (1982).

[25]P.-O. Löwdin, J. Chem. Phys. **19**, 1396 (1951).

[26]H. J. Monkhorst and J. D. Pack, Phys. Rev. B **13**, 5188 (1976).

[27]F. A. Cotton and G. Wilkinson, *Advanced Inorganic Chemistry* (Wiley, New York, 1980).

[28]A. Erbil, W. Weber, G. S. Cargill, and R. F. Boehme, Phys. Rev. B **34**, 1392 (1986).

[29]M. Scheffler, Physica B+C **146B**, 176 (1987).

[30]M. Hirata, M. Hirata, and H. Saito, J. Phys. Soc. Jpn. **27**, 405

(1969).
[31]See the article by A. D. Le Claire, in *Physical Chemistry,* edited by W. Jost (Academic, New York, 1970), Vol. X, p. 261, for a thorough discussion of correlation effects (as manifested by the binding strength between an impurity and a vacancy) in diffusion, especially with regards to impurity diffusion mediated by vacancies.
[32]S. T. Pantelides and C. S. Nichols (unpublished).
[33]C. S. Nichols and S. T. Pantelides (unpublished).
[34]C. Hill, in *Semiconductor Silicon 1981,* edited by H. R. Huff, J. R. Kriegler, and Y. Takeishi (Electrochemical Society, New York, 1981), p. 988.
[35]S. M. Hu, Appl. Phys. Lett. **27**, 165 (1975).
[36]G. B. Bronner and J. D. Plummer, J. Appl. Phys. **61**, 5286 (1987).

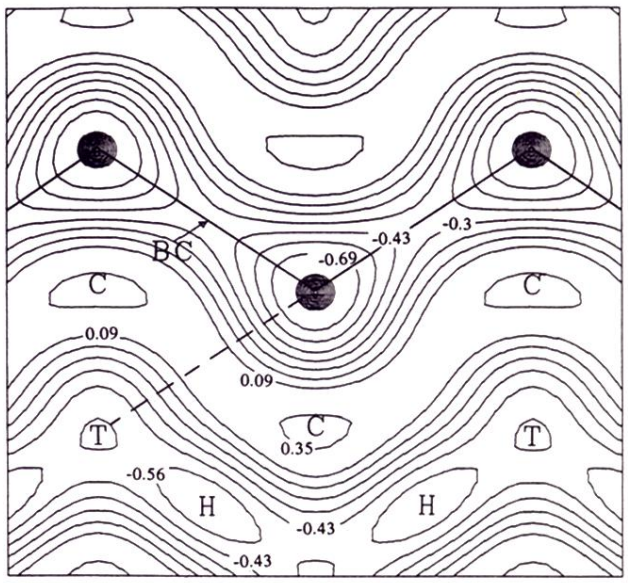

(a)

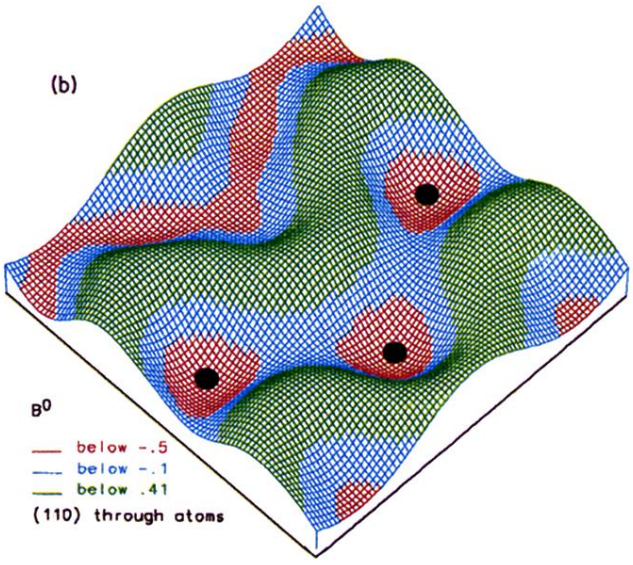

FIG. 3. Total-energy surface plots. (a) Total-energy contour plot depicting the migration of a neutral B interstitial through the Si crystal. The labeled sites are *T* (tetrahedral), *H* (hexagonal), BC (bond-center) and *C* (at the center of a rhombus formed by three adjacent Si atoms and the nearest *T*). The energy difference between contours is 0.13 eV. The dashed line is the kick-out pathway. The values of the contours near the channel regions are ≈ 0.2 eV higher than those reported in our previous publication (Ref. 16). This is a consequence of generating the surface with a higher plane-wave cutoff and does not change any of our conclusions based on that previous figure. (b) Perspective plot of the same process. The areas colored red are lowest in energy, blue are intermediate, followed by the highest-energy regions in green. Relaxations of the host atoms are not indicated in the figure, but are taken into account in the total-energy calculations.